Twenty-Sixth Symposium (International) on Combustion/The Combustion Institute, 1996/pp. 1531–1539

NUMERICAL SIMULATION OF THE DYNAMICS OF LARGE FIRE PLUMES AND THE PHENOMENON OF PUFFING

AHMED F. GHONIEM, ISSAM LAKKIS, AND MARIOS SOTERIOU

Department of Mechanical Engineering
Massachusetts Institute of Technology
Cambridge, MA 02139, USA

A vortex-based computational simulation of an axisymmetric fire plume is presented. The physical model accounts for unsteady buoyancy dynamics, conductive and convective heat transfer, and fast combustion. The effect of radiation is modeled by reducing the effective heat release from the combustion zone and raising the temperature of the evaporate from the pool. Numerical solutions are obtained using a modified vortex method in which the element vorticity is updated every time step according to source terms modeling the impact of gravity and pressure gradients in variable density flows. Attention is focused on the unsteady dynamics of the fire plume, or puffing, its dependence on the pool diameter, and the observed similarity between the unsteady behavior of isothermal and fire plumes. The numerical results show that, except for very low Reynolds numbers, fire and isothermal plumes oscillate at a frequency that depends most strongly on the pool diameter. The oscillations are accompanied by the shedding of large burning structures at a point located approximately one pool diameter above the ground. Most of the burning occurs within these structures, whose sizes are of the order of magnitude of the pool diameter. We find that the origin of the instability is a Kelvin–Helmholtz type mechanism of the vortex sleeve that forms at the interface between the fuel and air sides of the plume. The numerical results agree with experimental data on the shedding frequency, the average size of the structures and average flame height. We also find that while the buoyancy flux variation with height is different in fire and isothermal plumes, over a range of conditions, both cases have similar density fields near the pool and thus similar shedding characteristics.

Introduction

The environmental impact of massive natural and synthetic fires has received closer attention in recent years. The injection of large amounts of combustion products, including unburned hydrocarbons and soot, into the atmosphere can lead to severe air pollution problems locally and potentially on a regional scale [1,2]. Experimental studies have been conducted to determine the rate of burning and composition of products in pool fires, as laboratory models of massive fires, and examine the effect of scale on the fire characteristics [3]. Analytical and numerical modeling efforts have also focused on the same configuration. This paper reports some results from our program on the development and validation of a computational simulation of large fires.

Experimental observations show that three zones can be identified in a pool fire: the continuous flame zone, the intermittent combustion zone, and the inert plume zone [3]. The first zone is located near the pool, where fuel evaporation and air entrainment lead to the formation of an oscillating laminar, luminous flame envelope nearly attached to the pool. In the second zone, the flame surface fluctuates vigorously in the horizontal and vertical directions. The inert plume zone lies in the third zone where the flow is nonreacting and turbulent.

One of the most prominent features of pool fires is the periodic shedding of large burning structures, or puffs, within the intermittent zone [4]. Judging by similar phenomena in jet flames, this puffing is likely to be critical to the entrainment rate of ambient air and hence in determining the burning and heat-release rates, and the products' composition. Experimental results on pool fires of different sizes and fuels, including gaseous, liquid, and solid fuels, show that the puffing frequency is strongly dependent on the size of the pool and almost independent of the fuel type. The correlation $f = 1.5\sqrt{D}$, where the units of the puffing frequency, f, and the pool diameter, D, are Hz and m, respectively, has been suggested to summarize these data [3,4]. A Strouhal number $\tilde{S}t = fD/\sqrt{gD} = 0.5$ can be used to normalize this relationship, where g is the gravitational acceleration. It has been argued that the origin of oscillation is related to buoyancy dynamics, shear instability, buckling inviscid instability, formation of large scale structures, etc. [5–12].

It has been shown that, when instead of relying on liquid fuel evaporation, gases are injected into the pool, the burner exit fuel velocity V_0 has a small but finite influence on the puffing frequency. This influence is negligible for some diameters, provided that the exit velocity is larger than a critical value re-

quired to initiate pulsation [4]. Similar periodic motion was also observed in isothermal nonreacting buoyant plumes [4,7,13]. In this case, the puffing frequency scales with the pool diameter according to the following relationship: $S_t \sim F_r^{-m}$ where the Strouhal number is $S_t = fD/V_0$ and the Froude number is $F_r = V_0^2/gD$, with $m = -0.38$. Note that for a fire, $m = -0.57$. Clearly, more work is needed to elucidate the mechanisms and result of unsteady motion in fires.

The objectives of this work are to develop a computational fire plume model that incorporates the major physical mechanisms involved in determining the rate of burning and intensity of a fire (buoyancy dynamics, combustion, thermal convection, and radiation) and to use this model in assessing the environmental impact of massive fires. The origin of the fire plume model is a vortex-based computational model of a rising isothermal axisymmetric plume that was developed, validated, and applied to determine the nature of the oscillations observed during the slow release of buoyant gases in a quiet atmosphere [13]. The same model was used previously in wind-driven buoyant plume simulations [14]. These periodic oscillations were investigated over a wide range of parameters, such as the plume base diameter, the density ratio, and the initial velocity of the gas released. Good agreement with experimental measurements of the oscillation frequency has been shown. In this paper, we discuss the incorporation of combustion into the plume model, as a first step toward a comprehensive fire model, using a fast chemistry formulation, and use this model to investigate the oscillations observed in a fire plume.

Formulation

Experimental results suggest that under weak wind conditions, fire plumes remain nearly axisymmetric within the combustion zone [3,7,11]. For the purpose of developing the model and validating the results, we focus on the axisymmetric case. The governing equations are the continuity, momentum, energy, and species conservation equations and the equation of state. Combustion in non-premixed gases occurs when the fuel and oxidizer mix at the molecular level and react within thin zones. In fire plumes, chemical reaction rates are much faster than diffusion rates, and thus the process controlling the overall rate of burning is mixing (i.e., the entrainment of the fuel and oxidizer toward the reaction zone, followed by their interdiffusion within it). In this case, reactants can be considered to burn as soon as they come in contact; that is, the reaction zone collapses onto an infinitely thin interface and the fuel and oxidizer cease to coexist. In previous studies of reacting shear flow, we have found this to be a reasonable approximation when one is interested in estimating the burning rate and the impact of combustion on the flow field [15,16].

In this fast chemistry limit, the equations governing the distribution of species concentration and temperature can be simplified greatly using the Shvab–Zeldovich (SZ) variables. Assuming that the mass diffusion coefficients are all the same and the Lewis number is unity, these variables are constructed such that their governing equations are devoid of a source term, that is, if β is an SZ variable, it is governed by

$$\frac{D\beta}{Dt} = \frac{1}{P_e}\nabla^2\beta \tag{1}$$

where t is time, the Peclet number is $P_e = UD/\alpha$, and α is the thermal diffusivity taken here as a constant. Define the following SZ variables:

$$\lambda = Y_o - \phi Y_f,$$

$$\gamma = T - \frac{Q}{1+\phi}Y_p, \text{ and } \delta = Y_d \tag{2}$$

where Y is the species concentration, subscripts o, f, p, and d refer to oxygen, fuel, products, and diluent, respectively, ϕ is the mass stoichiometric coefficient, Q is the heat of reaction, and T is the temperature. If these variables can be normalized such that the resulting form has the same initial and boundary conditions, then Eq. (1) is solved only once for all SZ variables. We define this variable, ζ, the mixture fraction, as follows:

$$\zeta = \frac{\beta - \beta_o}{\beta_f - \beta_o} \text{ for } \beta = \lambda, \gamma, \text{ or } \delta \tag{3}$$

where subscripts o and f refer to the boundary conditions on the fuel and oxidizer sides of the plume, respectively. The boundary conditions for ζ are, on the fuel side, $\zeta = 1$, and on the air side, $\zeta = 0$. We nondimensionalize the variables with respect to a combination of $U = \sqrt{gD}$, D, atmospheric density and temperature, ρ_a, T_a, respectively.

Numerical Scheme

The numerical method used to simulate the evolution of the fire plume, the transport element method, is based on integrating the vorticity transport equation and the equations governing the gradients of the scalars, both reacting and conserved species, in their Lagrangian form [15,16]. This approach avoids the use of a grid and the discretization of gradients among neighboring points with its concomitant numerical diffusion problems. It also allows one to concentrate the computational points around zones of highest gradient and to move these elements to follow the gradients as they evolve. The

method has been described in numerous publications before and used to simulate other reacting flows; thus, it will not be discussed in detail here. However, since it is extremely useful in interpreting the numerical results, we will review the vorticity transport equation and discuss its implications.

In this axisymmetric flow, only the azimuthal vorticity, ω, is nonzero, where

$$\omega = \frac{\partial u}{\partial z} - \frac{\partial w}{\partial r}$$

where r and z are the horizontal radial and vertical axial directions, u and w are the velocity components in the two directions, respectively. Its governing equation is

$$\frac{D\omega}{Dt} + (\nabla \cdot \vec{u})\omega - \frac{u\omega}{r} = \frac{1}{\rho^2}\left(\frac{\partial p}{\partial r}\frac{\partial \rho}{\partial z} - \frac{\partial p}{\partial z}\frac{\partial \rho}{\partial r}\right) + \frac{1}{\rho^2}\frac{\partial \rho}{\partial r} + \frac{1}{R_e}\left(\nabla^2\omega - \frac{\omega}{r^2}\right) \quad (4)$$

where p is pressure. The second and third terms on the left-hand side and the last term on the right-hand side correspond, respectively, to vorticity modification caused by volumetric expansion, stretch as the ring radius changes, and molecular diffusion. None of these terms can create or destroy rotation, the total circulation associated with a material volume remains constant under their action (diffusion spreads vorticity over a larger material volume). On the other hand, the first two terms on the right-hand side can generate vorticity because of the interaction between the density gradient and the hydrodynamic pressure gradient and the density gradient and gravity. Starting from rest, they are responsible for converting potential energy into kinetic energy, as will be shown in the results.

The simulations were initiated by representing the sharp gradient between the plume and air using nine parallel layers of computational ring elements. As the layers moved upward and rolled into the large structures, more elements were introduced to maintain accuracy. Other numerical parameters, such as the time step and maximum distance between neighboring elements, were selected to ensure numerical convergence. The boundary conditions at infinity and on the ground were enforced exactly by selecting the appropriate Green functions for the velocity components. To curtail the growth in the number of computational elements, they were deleted as they passed through a "soft" boundary located about five pool diameters above the ground. Moving this boundary higher did not affect the numerical solution within the first flame height in any significant way.

Results and Discussion

We used the model described previously to simulate fire plumes over a range of conditions by varying the plume diameter and kinematic viscosity to change the Reynolds number, $R_e = UD/\nu$, where ν is the kinematic viscosity, and Richardson number,

$$R_i = \frac{\rho_a - \rho_f}{\rho_f}\frac{gD}{V_o^2}$$

independently. For most of the runs, transition to unsteadiness and puffing was observed. However, at very low values of R_e, the plume remained laminar and its shape resembled that of a converging chimney. At low R_e, puffing was irregular and the plume tended to relaminarize for some time before resuming its shedding. This was taken to indicate that shedding resulted from an intrinsic flow instability, most likely of a linear nature since only weak, numerically induced perturbations were allowed, which could be suppressed by viscous forces at low R_e. This does not indicate, however, that this is a viscous instability, as will be shown later. In the following, we examine the high Reynolds number cases only.

To investigate the fire plume dynamics, we present the results obtained for the following parameters: The molar masses and enthalpy of reaction are taken to correspond to a methane-air mixture: $M_f = 16$, $M_o = 32$, $M_d = 28$, $M_p = 26.62$, and $Q = 70$, while $\phi = 4.0$. The boundary conditions at the pool are, on the fuel side: $Y_f = 0.9$, $Y_o = 0.0$, $Y_p = 0.1$, and $Y_d = 0.0$, $\rho_f/\rho_a = 0.1975$ and $T_f/T_a = 3.0$, $V_0/U = 0.2$. The values on the air side are $Y_f = 0.0$, $Y_o = 0.2$, $Y_p = 0.0$, and $Y_d = 0.8$. With $R_e = 10^3$, these values correspond to $R_i = 101$. The heat of reaction was reduced from its adiabatic value to account for incomplete combustion and radiative losses, neither of which are represented explicitly in the physical model at this stage, and the initial temperature of the fuel was assumed to be higher than atmospheric temperature because of the intense radiative heating.

The unsteady calculation was initiated by following the material surrounding the interface between the rising fuel and air. As this interface rises, it forms the familiar mushroom cloud of buoyant flow. The mechanism leading to the formation of this mushroom can be understood by relating the geometry of the plume to the vorticity transport equation. Along the rising vertical surface of the plume, vorticity is generated because of the interaction between the density gradient and gravity. We note here that the plume gases are lighter than air as a result of their lower molecular weight and higher temperature. The latter is caused by the intense inward heating by the flames surrounding the plume. The rate of vorticity generation is proportional to the angle between the interface and the horizontal, that is, it is maximum when the interface is vertical. This vorticity rolls up close to the leading edge of the plume to form a vortex ring that endows the plume with the mushroom form.

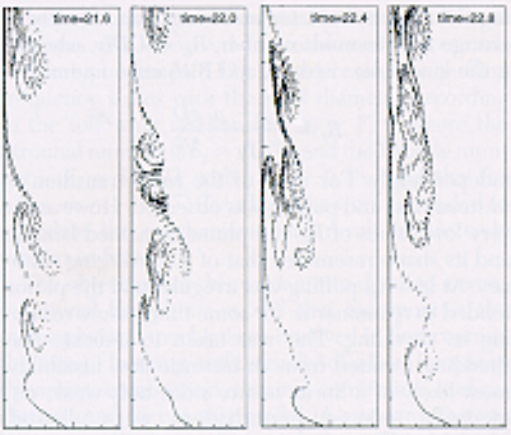

FIG. 1. The velocity vectors of the computational elements initially aligned with the contour of maximum density gradient.

Following this initial transient, the flow turns quasi-periodic with regular formation and separation of large vortices near the pool. A typical cycle involving the formation of these structures is shown in Figs. 1 and 2 in terms of the velocity vectors of the computational elements that coincide with the sharpest density gradient surface and the product concentration distribution, respectively. Near the fuel pool, a line passing through the computational elements convecting the sharpest density gradient can be thought of as the interface between the plume material and air (i.e., as the reaction interface). Figure 1, therefore, shows the extension and spiraling of the reaction front as large vortices form because of the roll-up of the vorticity generated along these fronts, while Fig. 2 shows the formation of the products along this surface and their accumulation inside the large structures.

The mechanism of periodic formation of these ring structures can be illuminated using Figs. 1 and 2. First, the vertical, buoyancy-induced acceleration of the plume gases causes the rising vertical interface to form a conical surface, along which vorticity is generated. The vorticity transport equation shows that the term $\langle \partial p/\partial r \rangle$ is the major source of vorticity in this field. This term is finite where the density interface is inclined with respect to the horizontal. The density contours for the fire plume are shown in Fig. 3, along with those obtained in the case of the isothermal plume. This shows that the distribution of vorticity along the rising interface is nonuniform in a way that depends on the local angle of the interface. The sense of this vorticity is clockwise.

An axisymmetric vortex sheet is known to be unstable to small perturbations via the Kelvin–Helmholtz mechanism, that is, small perturbations grow

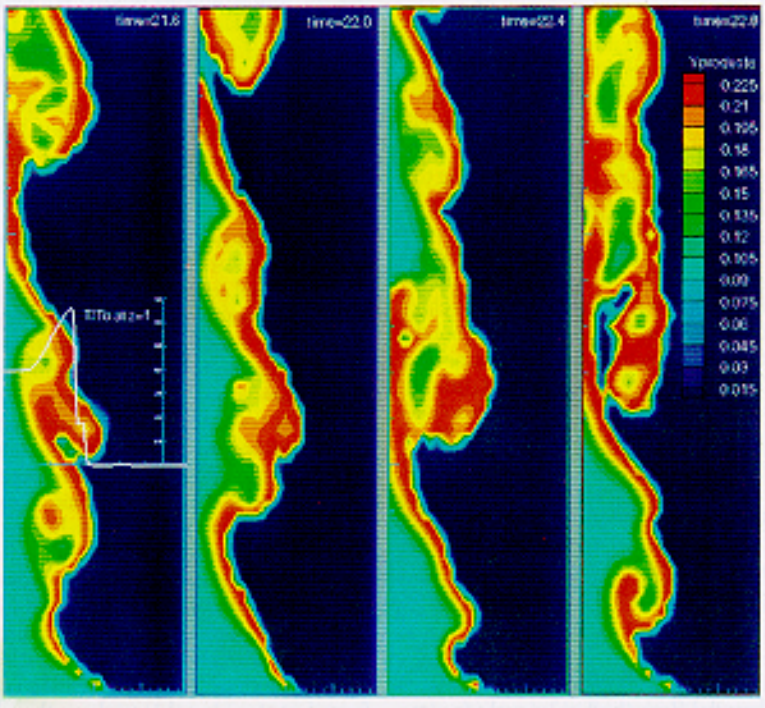

FIG. 2. The product mass fraction distribution in the fire plume.

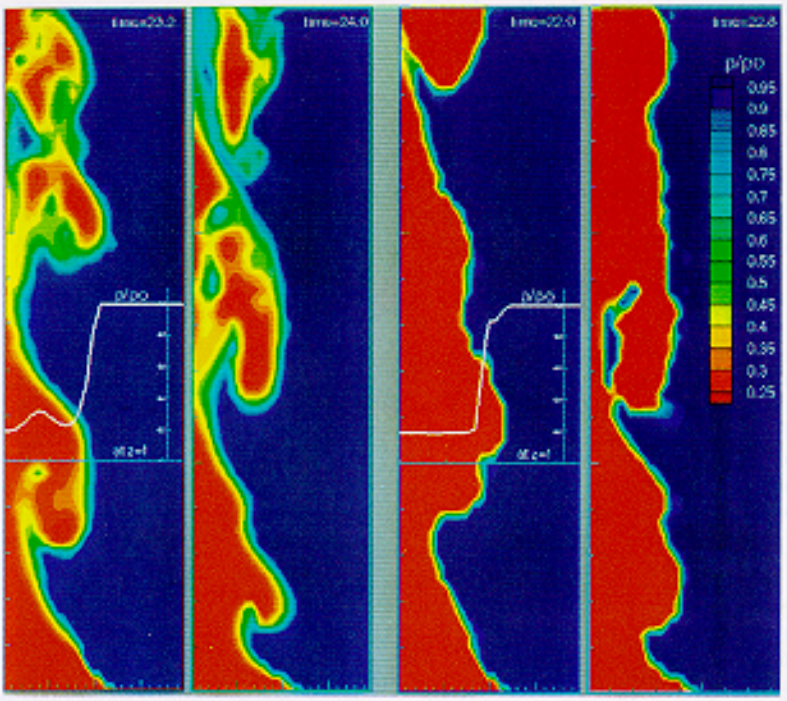

FIG. 3. A comparison between a reacting and an isothermal plume shown in terms of the density field in both cases.

along the sheet leading to its roll-up in the form of large vortical structures. The size of the structure is determined by the wavelength of the instability—in this case, it appears to be the distance between the pool and the plume neck, representing the length of the vortex sheet before roll-up. The Kelvin–Helmholtz instability is augmented by a Rayleigh–Taylor type instability as the roll-up pushes the hot gases outward and the cold air inward with respect to the interface. The result of these two effects is more vigorous growth of perturbations than in the presence of either mechanism. (The combined mechanism can still be thought of as an instability of a vortex sheet whose vorticity grows as a function of time.) The result of the roll-up is shown in Fig. 4 in terms of the vorticity distribution within the fire plume shown in Fig. 1.

The burning enhancement associated with the roll-up of the interface and the formation of large vortical rings or puffs is shown in Fig. 2 where the product mass fraction, or equivalently the temperature distribution, is depicted. The figure shows that most of the burning occurs following the extreme necking of the plume when the vortex ring reaches its maximum size and is nearly shed from the plume. The strong entrainment field induced by the ring brings in the necessary air to burn most of the plume fuel. That most of the burning occurs at this stage is shown in Fig. 5 where the fuel mass fraction distribution is depicted. To facilitate the discussion of the impact of puffing on the burning rate, we divide the vertical extent of the fire plume into three nearly equal zones, each extending one pool diameter in the vertical direction. Within the first zone, while the perturbation is growing, a rather slow fuel consumption rate occurring on the outer edge of the plume interface is observed. Within the second zone, where the large vortex separates from the plume, one observes a very fast rate of fuel consumption occurring within the large structure where flame winding and air entrainment is strongest. At the third zone, while most of the fuel has been consumed, pockets of high-fuel concentration still survive within the large eddies and close to the centerline of the plume.

Many of the observations reported in experimental studies [3,7,11] support the results of our numerical simulations despite the simplifying assumptions incorporated in our model. Indeed, a sharp necking of the rising plume, followed by the formation of a large burning structure that is periodically shed from the pool, is seen in the flow visualization. The burning structure, whose extent in the horizontal direction is close to one plume diameter and that appears at nearly one plume diameter above the pool surface, can be discerned clearly. The total flame height, that is, the point at which most of the fuel has burned, fluctuates between two and three plume diameters, similar to our results. Finally, the

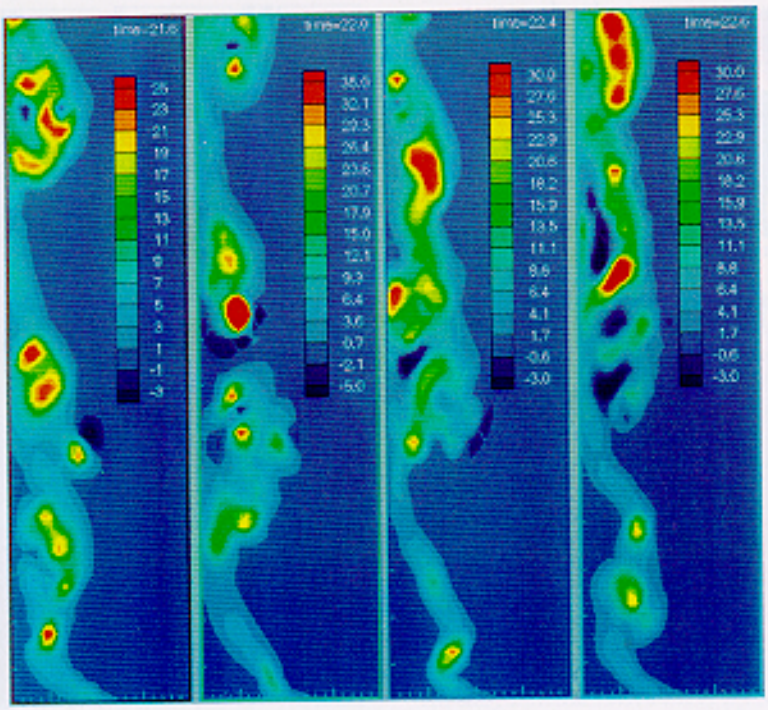

FIG. 4. The vorticity distribution in the fire plume.

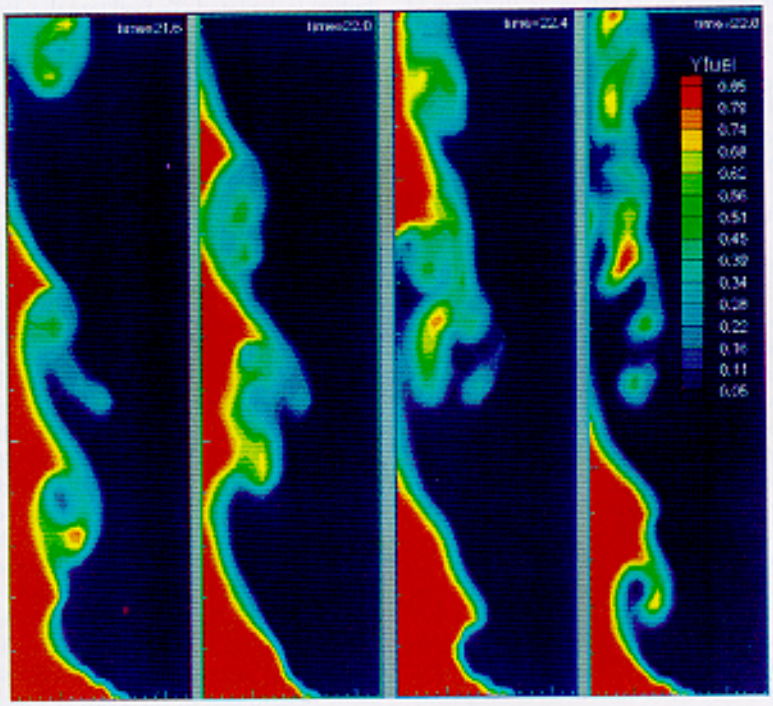

FIG. 5. The fuel mass fraction distribution in the fire plume.

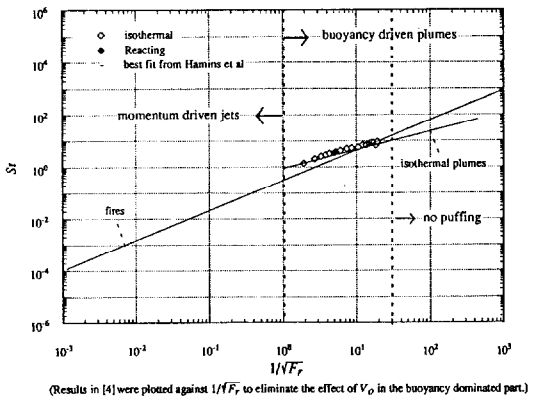

FIG. 6. Puffing frequency dependence on the plume diameter for fire and isothermal plumes.

shedding frequency predicted by our simulation, which is obtained by analyzing the velocity spectrum at a number of points above the pool, is $S_t = 3.6$, which for $D = 0.1$ m corresponds to $f = 7.2$ Hz. This value agrees well with the experimental fit shown in Fig. 1 in Ref. 4. Similar agreement was found for other simulations at different conditions.

One of the interesting observations on fire plumes is the qualitative similarity between their puffing and that of isothermal plumes [4,7]. As mentioned previously, both oscillate at a frequency that depends on a negative power of the Froude number. While the exponents are different in both cases, as shown in Fig. 6, which is taken from the compiled results in [4], there is a range of overlap between the correlations describing puffing in both cases. We simulated isothermal plumes over a wide range of conditions and obtained shedding frequencies very close to those reported experimentally [13]. Thus, there seems to be strong evidence that while the exact dependence of the shedding frequency on the pool diameter may be slightly different in the isothermal and reacting plume cases, over a rather wide range of conditions the values of the two cases overlap (i.e., there must be strong resemblance in the controlling mechanism).

To explain the origin of the similarity, we reexamine Fig. 3 in which the density distribution of both the reacting plume and an isothermal plume obtained at the same density ratio, Reynolds and Froude numbers are shown. The figure shows a strong similarity between the density distributions for both cases near the pool, namely, before the extreme necking and shedding of a large structure. This similarity, which is in sharp contrast with the corresponding temperature fields (Fig. 2) is a manifestation of the fact that the density field depends on both the temperature and the molecular weight of the mixture.

On the other hand, and in agreement with the argument advanced by Delichatsios [17] to explain the difference between the two cases, the buoyancy flux, or flow rate of low density fluid increases upwards in the fire plume while it remains constant in the nonreacting plume. As indicated in our earlier discussion, it is the early stages, within the first 1–2 pool diameters, that seem to determine the shedding dynamics in these plumes. This last remark is essential in explaining the qualitative, and within a reasonably wide range, quantitative agreement between the shedding frequency in both cases. It must be added that at extreme values of the Froude number, the shedding frequency and its dependence on the pool diameter can differ substantially in both cases. This is because at these extremes, the density distributions, even at the early stages, will be different in both cases; for example, in the fire plume, it may take longer to establish a low density fluid flux similar to that observed in the isothermal plume.

Conclusions

The development of a computational simulation of a fire plume requires the incorporation of buoyant flow dynamics, combustion, thermal convection, and radiation. In this work, we simulate the unsteady axisymmetric flow dynamics directly while assuming infinitely fast chemistry and model radiation by reducing the heat of reaction of the mixture, assuming that the initial temperature of the fuel is higher than the atmospheric value and using a gaseous fuel pool. To maintain computational efficiency, a Lagrangian numerical scheme is used to perform the simulations. Results of the numerical simulation of an axisymmetric reacting plume show the following:

1. The computational model is capable of predicting the puffing frequency, illuminating the dynamics leading to puffing, and the underlying fields of major species, temperature, and dynamic variables.
2. Puffing results from an intrinsic flow instability associated with the formation of an axisymmetric vortex sheet along the boundary between the inner hot gases and the outer colder gases. Vorticity is generated by the presence of a radial density gradient in a gravity field. The instability leading to puffing is associated, however, primarily with the properties of the axisymmetric vortex sheet.
3. Puffing also occurs in isothermal plumes since similar density gradients exist. The similarity between the density distributions at the early stages of both reacting and in isothermal plumes is due to governance by both the temperature distribution and the molecular weight of the mixture. While in the reacting plume, the temperature increases and then decreases sharply at the plume interface, differences in molecular weights lead

to a density distribution that resembles that encountered in inert plumes.

Acknowledgments

This work is supported by a grant from the Building and Fire Research Laboratory of the National Institute of Standards and Technology. Computer Resources are provided by the Pittsburgh Supercomputer Center.

REFERENCES

1. Evans, D., Baum, H., Mulholland, G., Bryner, N., and Forney, G., "Smoke Plume from Crude Oil Burns," NISTIR Report, NIST, 1989.
2. Zhou, H. and Ghoniem, A. F., First Annual Report on the Development of a Computational Fire Plume, BFRL-NIST, 1994.
3. Zukoski, E. E., "Properties of Fire Plumes," in *Combustion Fundamentals of Fires* (Cox, G., Ed.), Academic Press, New York, 1995, pp. 101–220.
4. Hamins, A., Yang, J. C., and Kashiwagi, I: *Twenty-Fourth Symposium (International) on Combustion,* The Combustion Institute, Pittsburgh, 1992, pp. 1695–1702.
5. Weckman, E. J. and Sobesiak, A., *Twenty-Second Symposium (International) on Combustion,* The Combustion Institute, Pittsburgh, 1988, pp. 1299.
6. Bouhafid, A., Vantelon, J. P., Joulain, P., and Fernandez-Pello A. C., *Twenty-Second Symposium (International) on Combustion,* The Combustion Institute, Pittsburgh, 1988, pp. 1299–1310.
7. Cetegen, B. M. and Ahmed, T. A., *Combust. Flame* 93:157–184 (1993).
8. Hertzburg, M., Cashdollar, K., Litton, C., and Burgess, D., Report No. 8263, Bureau of Mines, U.S. Department of Interior, 1987.
9. Sibulk, M. and Hansen, A. G., *Combust. Sci. Technol.* 10:85–92 (1975).
10. Byram, G. M. and Nelson, R. M., *Fire Technol.* 6(2):102–110 (1970).
11. Zukoski, E. E., Cetegen, B. M., and Kubota, T., *Twentieth Symposium (International) on Combustion,* The Combustion Institute, Pittsburgh, 1984, pp. 361–366.
12. Bejan, A., *J. Heat Transf.* 113:261–262 (1991).
13. Lakkis, I. A. and Ghoniem A. F., Annual report on the Development of a Computational Model for Fire Plume, BFRL-NIST, 1995.
14. Zhang, X. M. and Ghoniem, A. F., *Atmospheric Environ.* 27A(15):2295–2311 (1993).
15. Soteriou, M. C. and Ghoniem, A. F., *Combust. Sci. Technol.* 105:377–397 (1995).
16. Soteriou, M. C. and Ghoniem, A. F., *Twenty-Fifth Symposium (International) on Combustion,* The Combustion Institute, Pittsburgh, 1994, pp. 1265–1272.
17. Delichatsios, M. A., "Gravitational Fluctuations in Pool Fires and Pool Buoyant Flows," A technical note submitted to *Combust. Sci. Technol.* 1994.

COMMENTS

Viswanath R. Katta, Innovative Scientific Solutions, Inc., USA. There is a major difference between the plume and the plume flame. In the former, temperature and velocity decay with radial distance. However, in the plume flames, fuel diffuses radially outward from the plume jet and burns in the flame zone. This particular feature of the flame makes the velocity of the plume flame decay faster than the temperature; which, consequently puts the thermal layer in a relatively lower velocity regime of the velocity profile. Naturally, lower velocity results in lower frequency. Therefore, for the same exit velocity, flickering frequency associated with the plume will be higher than that of the plume flame. If the jet velocity is low, then differences in the instability mechanisms play a big role.

Author's Reply. The authors are delighted that their provocative statement regarding the closeness of shedding frequency of isothermal and reacting plumes, within a certain range of Fronde number, can be explained by the similarity between the density fields in both cases, has generated so much discussion. In order to support this statement, one need only remember, as shown by the results in Figs. 2, 3 and 5, that the onset of the instability leading to the shedding or puffing, occurs very close to the pool, within a pool radius above the ground (this is well supported by experimental data, see Ref. 3). Within this length, very little combustion has taken place and the density gradient is established essentially by the interface between the rising plume material and air. Thus, even in the reacting plume, the instability is initiated at the very early stages within the shear layer across which the density difference is that between the fuel evaporate and air.

Within the range of Fronde number, which according to Ref. 4 spans nearly 5 orders of magnitudes, discussed in the paper conditions seem to be right for the two density fields to be so similar that the puffing frequencies of both cases are nearly the same. Incidently, and contrary to the comment, the puffing frequency of the reacting plume could be higher or lower than that of the isothermal plume depending on the value of the Fronde number.

•

M. A. Delichatsios, FMRC, USA. The fact that the two correlations (for Helium flow and pool fires) show a region where they have frequency values very close with each other does not mean that physics of oscillations are the same for the two situations. The difference in physics for

these two situations is explained in a paper to be published shortly [1].

REFERENCE

1. Delichatsios, M. A., *Combust. Sci. Technol.*, in press, 1996.

Author's Reply. We agree that several aspects of the physics of the isothermal plume and the reacting plume differ since, as pointed out by Delichalios in the referenced note, the buoyancy flux is constant in the former and increases within the flame height in the latter. However, as we pointed out in our response to the first comment, the onset of the instability leading to puffing occurs very close to the pool and before any significant change in the buoyancy flux due to combustion. This is supported by the density fields shown in Fig. 3 in which, within the early stages, the density gradients are nearly identical. As such, for $10^{-1} < 1/\mathrm{Fr} < 10^{5}$, we observe nearly the same values of St for both cases. We should add that our results confirm the theory that puffing is due to an intrinsic instability of the shear layer developing between the plume gas and air, and as has been illustrated in previous studies of similar instabilities, the most unstable frequency is a strong function of the density ratio across the shear layer.